AD-A152 252 HIGH RE SEPARATED FLOW SOLUTIONS USING THE NAVIER-STOKES AND APPROXIMATE.. (U) YALE UNIV NEW HAVEN CT DEPT OF COMPUTER SCIENCE M NAPOLITANO JAN 85 1/1

UNCLASSIFIED YALEU/DCS/RR-358 N00014-82-K-0184 F/G 20/4 NL

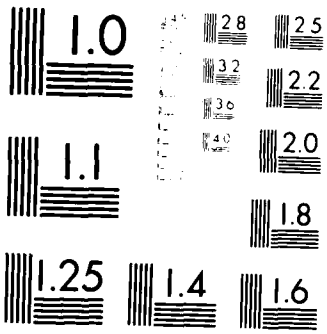

High Re Separated Flow Solutions Using the Navier-Stokes and Approximate Equations

Michele Napolitano[1]

Research Report YALEU/DCS/RR-358
January 1985

YALE UNIVERSITY
DEPARTMENT OF COMPUTER SCIENCE

Abstract The present study is concerned with the numerical simulation of high Reynolds number weakly separated steady laminar flows. It is shown that a "well designed" code can solve the complete Navier-Stokes (NS) equations and the "more suitable!" parabolized Navier-Stokes (PNS) equations with the same convergence rate, so that solving the full NS equations is recommended when dealing with a new problem. Furthermore, solutions to the classical boundary layer equations in their vorticity-stream function form are obtained, which are regular thru the separation point, i. e., do not encounter the Goldstein singularity at separation. Finally, for a very typical high Reynolds number weakly separated flow, it is shown that, in the presence of non negligible skewness in the body oriented computational grid, a PNS-type approximation still provides very reliable solutions, whereas an interacting boundary layer-type model is plagued by severe errors.

X

per

Ltr

A-1

High Re Separated Flow Solutions Using the Navier-Stokes and Approximate Equations

Michele Napolitano[1]

Research Report YALEU/DCS/RR-358
January 1985

[1] Istituto di Macchine, Universitá di Bari, via Re David 200, 70125 Bari, Italy

Work supported in part by ONR Grant N00014-82-K-0184 and in part by MPI and CNR.

Introduction

High Re (Reynolds number) attached flows have been computed routinely for several decades using the classical boundary layer (BL) theory of Prandtl: the inviscid flow past the body of interest is computed at first and then the BL equations are solved, using the inviscid pressure gradient as a datum, to evaluate the skin friction and thus the aerodynamic drag. Eventually, the displacement thickness obtained by the BL equations is added to the body to provide an "augmented body" around which the inviscid flow is recomputed and so on, according to a rigorous asymptotic expansion theory provided by Van Dyke [1].

Unfortunately, the classical BL theory breaks down in the presence of flow separation, so that a lot of computational effort has been devoted to the development of numerical methods for solving the Navier-Stokes (NS) equations. However, theoretical studies (see, eg, [2]) as well as numerical investigations (see, eg, [3, 4]) have shown that, for high Re weakly separated flows, the terms contained in the classical BL equations are sufficient to model the flow field even in the separated region. It is now understood that the failure of the classical BL theory (when the pressure gradient is prescribed) is due to the lack of upstream propagation required to account for the "elliptic" nature of the separation phenomenon; and in fact, solutions to the BL equations, which are regular thru the separation point, have been obtained by prescribing either the displacement thickness [5], or the wall shear [6], in place of the pressure gradient.

More in general, useful solutions for high Re separated flows can be obtained from an appropriate subset of the NS equations, provided that the "elliptic" nature of the strong viscous inviscid interaction phenomenon is correctly accounted for. Among the many such approximate equations used in the literature, the most widely employed and investigated appear to be the so-called parabolized Navier-Stokes (PNS) and interacting boundary layer (IBL) equations. Starting from the NS equations written in a body oriented orthogonal coordinate system the PNS equations are easily obtained by dropping the diffusion terms in the streamwise direction. The IBL equations are obtained instead by coupling the classical BL equations with a pressure interaction law, which accounts for the variations in the inviscid (outer) pressure field induced by the viscous effects. The PNS equations can then be considered from an asymptotic point of view as a composite set of equations uniformly valid in both the inner (viscous) and the outer (inviscid) regions and therefore "equivalent" to the complete NS equations. The IBL equations are valid instead only in the viscous region, whereas the inviscid flow is computed by means of another set of equations; and the viscous-inviscid interaction phenomenon is accounted for iteratively, e. g., by solving the inviscid and viscous flow equations using the same displacement thickness

(prescribed appropriately) and repeating the calculations until both sets of equations provide the same pressure distribution along the displacement body. For the case of the vorticity-stream function equations, of interest here, the PNS equations are obtained by simply dropping the streamwise diffusion term in the vorticity equation, so that they are also known in the literature as the parabolized vorticity (PV) equations [3, 4]. The classical BL equations are obtained by dropping the streamwise derivative(s) also in the stream function equation, according to the asymptotic order of magnitude analysis of Prandtl, and the IBL equations are therefore obtained by coupling the BL equations in the viscous region (where the vorticity is nonzero) with the Laplace equation for the stream function in the inviscid region, so as to allow for the viscous-inviscid interaction phenomenon.

To date, a large number of numerical studies have shown that for many flow fields of practical interest, namely for all of the high Re weakly separated flows, the PNS or even the IBL equations provide a satisfactory answer, so that it would appear as an unnecessary waste of computational effort to resort to the complete NS equations, see, e. g., [7-10]. Furthermore, due to the pioneering theoretical work of Smith and Chen [11-13], it starts to appear more and more evident that the IBL equations are capable of predicting also the massive separation phenomenon and the stall, as it has also been shown numerically by Rothmayer and Davis [14].

However, the NS equations still remain the only numerical tool capable of verifying the correctness of the new asymptotic theories and, if solved properly, they require a computational effort which is of the same order of magnitude as that required by the PNS, if not by the IBL equations. In fact, although obvious, it does not seem to be generally understood that a numerical method for solving the NS equations for high Re weakly separated flows has to be very similar in nature to efficient PNS or IBL codes; i. e., it has to account for downstream-propagation and transversal-viscous effects implicitly and only for the upstream-influence in an iterative fashion. For such a code, the convergence rate will be the same (see, e. g., [10]) whether only the terms present in the PNS (or even the IBL) equations are computed or all of the terms in the complete NS equations are accounted for; and the extra computational cost required to compute the negligible streamwise diffusion terms will be insignificant with respect to that required to solve the PNS equations. But what, if one of these term is essential to model a locally important phenomenon? It is worth pointing out that many IBL codes only solve the BL equations (iteratively) in the viscous region, with a far field condition, obtained by computing the inviscid flow past the displacement body according to thin airfoil theory, accounting for the interaction phenomenon (see, e. g., [14]). These methods, of course, may require significantly less computational effort than codes solving the complete NS equations, especially for the case of

supersonic outer flow.

The aim of this work is to demonstrate that for high Re weakly separated flows, a well designed NS-PNS code can compute the NS or the PNS equations with exactly the same convergence rate and at about the same computational cost, so that, when solving a novel problem, the additional cost of carrying all of the terms contained in the NS equations is minimal and certainly justified by the fact that the model employed accounts for all meaningful phenomena. Of course, by no means it is implied that solving the NS equations by "brute force" is an appropriate investigating tool! Asymptotic analyses are essential indeed, to prescribe appropriate computational grids and the location and type of the farfield boundary conditions, as well as to validate (and be validated by) numerical solutions.

Furthermore, the present study aims to demonstrate that, when solving the vorticity stream function equations, solutions for high Re separated flows, which are regular thru the separation point, can be obtained by solving, in the viscous region, simply the classical BL equations, namely, by dropping the streamwise derivatives also in the stream function equation. In particular, for the case of the high Re flow in a symmetric channel with a smooth expansion proposed by Roache [15], which is of parallel type, namely has negligible streamwise curvature effects, these solutions of the BL equations will be shown to be in very good agreement with results of the PNS and of the complete NS equations.

Finally, for a very typical high Re weakly separated flow, already studied by several authors [7-10], in the presence of skewness of the body fitted coordinate system, it is shown that PNS-type equations still provide results in good agreement with the complete NS solutions, whereas IBL-type equations experience marked errors due to the incorrect representation of the streamwise pressure gradient.

Governing Equations and Numerical Technique

The vorticity-stream function equations are given in a system of body-oriented curvilinear coordinates as:

$$\omega_t + (\psi_\eta\,\omega_\xi - \psi_\xi\omega_\eta)/J - (\underline{\alpha\omega_{\xi\xi}} - \underline{2\beta\omega_{\xi\eta}} + \gamma\omega_{\eta\eta} + \sigma\omega_\eta + \underline{\tau\omega_\xi})/\mathrm{Re} = 0 \qquad (1)$$

$$\underline{\alpha\psi_{\xi\xi}} - \underline{2\beta\psi_{\xi\eta}} + \gamma\psi_{\eta\eta} + \sigma\psi_\eta + \underline{\tau\psi_\xi} + \omega = 0 \qquad (2)$$

In eqns (1-2) -ω is the vorticity, ψ is the stream function, ξ and η are the streamwise and transversal coordinates, t is the time, subscripts indicate partial derivatives and J, α, β, γ, σ and τ are the jacobian and the scale factors of the mapping of the physical coordinates x, y into the computational coordinates ξ, η [16]. Furthermore, the terms underlined are those which are to be dropped to provide the PNS equations and those underlined with a broken line are the additional terms which also need to be dropped to obtain the classical BL equations. Of course, BL theory strictly requires the use of orthogonal coordinates, for which β in eqns (1-2) is identically zero. However, the PNS equations have been shown to be valid also in a "Mildly Nonorthogonal Coordinate System" [10], so that the aforementioned definition of PNS and BL equations is used here. Eqn (2), with the vorticity term eliminated, obviously is the Laplace equation for the stream function governing the inviscid irrotational portion of the flow field.

In the present study the incremental block-line Gauss-Seidel method proposed in Ref. 17 is used as an efficient numerical tool for solving eqns (1-2) numerically. The governing equations are discretized and linearized in time using a two level implicit Euler scheme and the delta approach of Beam and Warming [18] to give:

$$\Delta\omega/\Delta t + (\psi_\eta{}^n\,\Delta\omega_\xi + \omega_\xi{}^n\Delta\psi_\eta - \psi_\xi{}^n\Delta\omega_\eta - \omega_\eta{}^n\Delta\psi_\xi)/J$$
$$- (\alpha\Delta\omega_{\xi\xi} + \gamma\Delta\omega_{\eta\eta} + \sigma\Delta\omega_\eta + \tau\Delta\omega_\xi)/Re =$$
$$- [(\psi_\eta{}^n\,\omega^n)_\xi - (\psi_\xi{}^n\omega^n)_\eta]/J + (\alpha\omega_{\xi\xi}{}^n - 2\beta\omega_{\xi\eta}{}^n + \gamma\omega_{\eta\eta}{}^n + \sigma\omega_\eta{}^n + \tau\omega_\xi{}^n)/Re \qquad (3)$$

$$\Delta\psi/\Delta t - \alpha\Delta\psi_{\xi\xi} - \gamma\Delta\psi_{\eta\eta} - \sigma\Delta\psi_\eta - \tau\Delta\psi_\xi - \Delta\omega =$$
$$\alpha\psi_{\xi\xi}{}^n - 2\beta\psi_{\xi\eta}{}^n + \gamma\psi_{\eta\eta}{}^n + \sigma\psi_\eta{}^n + \tau\psi_\xi{}^n + \omega^n \qquad (4)$$

where a relaxation-like time derivative has been added to the stream function equation to parabolize it, Δt is the time step (which can be different in eqns (3) and (4) and can also vary at every iteration), $\Delta\omega = \omega^{n+1} - \omega^n$, the superscripts n+1 and n indicating the new and old time levels t^{n+1} and t^n, etc. Notice that the mixed derivatives are evaluated at the old time level t^n, i. e., explicitly and therefore do not appear in delta form. The presence of such terms in the vorticity equation of the complete NS equations (when a nonorthogonal computational grid is employed) can be critical insofar as they may reduce the stability and therefore the convergence rate of the numerical method.

Eqns (3-4) are then discretized in space using second-order-accurate central differences throughout - except for the incremental convective terms of the vorticity equation in the left

hand side of eqn (3), which are approximated using first-order-accurate upwind differences - and solved by a classical line Gauss-Seidel relaxation method, marching from left to right (see [17], for details). It is noteworthy that by using a deferred corrector strategy for the advection terms in eqn (3), which are approximated using upwind differences in the LHS and central differences in the RHS, upstream propagation is allowed, although explicitly, even when solving the classical BL equations, i. e., when all of the elliptic terms are dropped from the equations.

Results

The first problem considered in this study is the weakly separated channel flow proposed by Roache [15]. The geometry of the channel, together with the appropriate boundary conditions and the orthogonal 41x21 grid employed in this study is given in Figure 1 for the case Re = 10. Roache has shown that if the length of the channel is increased proportionally to Re, for Re >> 1, the solution takes on a quasi-self-similar form; i. e., the skin friction at the wall becomes independent of Re, when plotted versus x/Re. As such, the present problem is very suitable to assess the capability of a numerical technique to compute high Re weakly separated flows; more importantly, for Re >> 1 , the length of the separation bubble is found to increase proportionally to Re, whereas its height remains constant, so that, from an order of magnitude analysis, it can be argued that:

$$u = O(1) \tag{5}$$

$$v = O(1/Re) \tag{6}$$

$$\partial/\partial y = O(1) \tag{7}$$

$$\partial/\partial x = O(1/Re) \tag{8}$$

where O( ) indicates the standard asymptotic order of magnitude symbol. If, for large values of Re, equations (5-8) are true, than the PNS equations and even the classical BL equations should provide results practically coincident with those computed using the complete NS equations. The same code was therefore used to solve the three aforementioned sets of equations, for the case Re = 10^6, using the 41x21 mesh depicted in Figure 1.: the results for the vorticity at the wall were found to be identical (to machine accuracy, i. e., 6 significant digits), with no indication of the singularity at separation appearing when solving (iteratively) the classical BL equations. In order to better assess this last very important issue, as well as the accuracy of the present numerical results, a grid refinement study was conducted in both the x (quasi-streamwise) and the y (quasi-normal) directions, using meshes with 61x21, 81x21, 41x41 and 41x61 gridpoints,

the horizontal mesh-size being always uniform and the normal one increasing at a constant rate equal to 1.1, starting from the wall. The results of the mesh refinement studies are given in Figures 2 and 3 as the vorticity distributions along the wall: it clearly appears that the basic 41x21-mesh solution is already "exact", to plotting accuracy. Again, the NS, PNS and BL results coincided to machine accuracy in all cases and no indication of singularity at separation was ever encountered. It is noteworthy that for the present flow case, the length of the channel being equal to Re/3, the longitudinal step size is always several orders of magnitude larger than the order-one BL thickness, so that also an "ill-posed" marching method could possibly recover the correct solution [15], by swamping out all branching solutions due to truncation errors. Therefore, the Re = 100 flow case was also considered in this study: the BL equations were solved using two meshes having 81x21 and 161x21 gridpoints. The two solutions were found to coincide with each other and (after proper scaling) with those of Figures 2 and 3, to plotting accuracy. In conclusion, the BL equations, when solved in an iterative way which allows for upstream propagation, clearly do not encounter any singularity at the separation point. This result is not surprising insofar as the value of the stream function is prescribed as a boundary condition at the centerline of the channel; such a condition is equivalent to prescribing the displacement thickness in the pressure-velocity BL equations, which has been shown to produce separated flow solutions which are regular thru the separation point [5]. Finally, the convergence rate for all three sets of equations and the same mesh was always found to be identical and is provided in Figure 4, where the average variation of the vorticity between two successive iterations is plotted versus the iteration number. It is noteworthy that the convergence rate of the method is remarkable and just about independent of the mesh employed for the calculations; this last result is very atypical of any relaxation method, so that it is most likely due to the one-dimensional (parallel) nature of the flow.

In order to compare the present NS and PNS solvers for an "extreme" situation, the Re = 10 flow was also considered. For such a case, the geometry is considerably distorted, see Figure 1, and the Reynolds number is very low, so that it is reasonable to expect large differences between the NS and the PNS solutions, whereas the BL equations are obviously meaningless. However, the present NS and PNS solutions still provide wall vorticity distributions, see Figure 5, which are qualitatively very similar. This result provides further evidence of the broad range of applicability of the PNS equations.

For all of the calculations above, an appropriate Couette flow was used at every longitudinal location as the initial condition and the time step was chosen equal to Re, initially, and then updated after every iteration by dividing its initial value times the vorticity error. Therefore, for

the particular case Re = 10^6, the time steps were so large that the time derivatives played no role in the computational process.

A second well known high Re weakly separated flow problem was considered in the present study, namely the flow in a symmetric diffuser already studied by several authors [7-10], in order to compare the NS and PNS solutions for a more general (non-parallel) flow and in the presence of local skewness of the computational grid, as well as to assess the efficiency of the present code with respect to several high Re weakly separated flow solvers [7-10]. Two flow cases were considered, whose geometry and computational grid are given in Figures 6a and 6b. In both cases the nondimensional semiheight of the channel is equal to 1, the Reynolds number, defined with respect to such a reference length and to a unitary velocity, is equal to 6250 and the inlet flow is a Blasius boundary layer produced by a flat plate whose leading edge is two units before the entrance of the channel; also, the midplane of the channel is located at y = 1, whereas the (bottom) wall, $y_w(x)$, is prescribed as follows:

$$y_w(x) = \begin{cases} 0 & \text{for } -1 < x < 0 \\ A[x^2(3 - 2x)] & \text{for } 0 \leq x \leq 1 \\ A & \text{for } 1 < x < x_{out} \end{cases} \qquad (9)$$

In the first flow case A = - 0.08 and x_{out} = 3, whereas in the second more severe one, A = - 0.16 and x_{out} = 6. The computational meshes employed in this study contain 81 and 71 equally spaced gridpoints in the x direction, respectively, and 41 gridpoints in the y direction, stretched in such a way that the vertical mesh size grows at a constant rate of 1.08, starting from the wall. In Figure 6a only every other gridline is plotted, whereas in Figure 6b all of the vertical coordinate lines are shown. The mesh in Figure 6a was chosen fine enough to provide reasonably accurate answers to compare with previously published results, whereas the mesh in Figure 6b is not considered adequate to provide accurate solutions, but valuable to provide a meaningful one-to-one comparison between NS and PNS results obtained using the same numerical method and mesh. It is noteworthy that in the range $0 \leq x \leq 1$, the mesh is nonorthogonal, so that the mixed derivatives in eqns (1-4) may be expected to play a considerable role, especially for the second more severe flow situation. For both flow cases, results were obtained using the same computer code to solve the NS and the PNS equations. The initial condition was taken to be the inlet boundary condition in the entire flow field. Symmetry was enforced by prescribing the value of the stream function at the center of the diffuser (y = 1), where a zero vorticity was also prescribed. At the wall the standard no-slip zero-injection conditions were imposed and, finally, the BL equations were solved at the outlet station, with the first derivatives evaluated as three-point second-order-accurate backward differences. The initial time step was taken to be equal to

0.1 for the vorticity equation and 1000 for the stream function equation. After every iteration the time steps were adjusted by dividing the initial values by the average vorticity and stream function variations (residuals), respectively. An overrelaxation factor [8] of 1.5 was also used, for the stream function equation only. All of these values are the first and only ones used, so that no optimization of the convergence rate of the method was pursued. For the first flow case, IBL-type equations were also solved, by dropping the streamwise derivatives also in the stream function equation, in the viscous region, while retaining it in the outer inviscid flow (namely, in the upper half of the computational gridpoints).

The results for the first flow case are given in Figures 7 and 8, where the convergence history for the NS and PNS equations and the vorticity distributions along the wall for all of the three sets of equations are given, respectively. The corresponding results for the second flow case are given in Figures 9 and 10, respectively. From the results in Figures 7-10 the following conclusions emerge. The NS and PNS equations provide practically identical results and converge at the same rate. The IBL-type equations are plagued, instead, by local errors near the curvature discontinuities at the wall, where the pressure gradient induced by the inviscid turning of the streamlines is not accounted for correctly. It is noteworthy that for the second flow case the IBL-type equations still converge without difficulties, but the final solution is completely destroyed by spatial oscillations produced by the more severe curvature discontinuities. Also, the convergence rate of the IBL-type equations, not reported in Figures 7 and 9, is slightly slower than that of the NS and PNS equations, due to the local larger gradients to be computed.

The present solution given in Figure 8, after proper scaling, is found to be in reasonable agreement with those of Edwards and Carter [7] and of Hoffman [10], but predicts a slightly longer separation region. The PNS equations were therefore solved using a finer 121x61 mesh; the results, also given in figure 8, are almost identical to those obtained using the coarser mesh. The present solutions are thus considered "correct", to plotting accuracy, and the slight discrepancy with the aforementioned solutions is believed to be due to their first-order-accuracy in the streamwise direction. For the second flow case, these authors do not report the skin friction distribution. However the length and position of the separated region can be compared using the streamlines plot of Ref 7. Again, the present solutions predict a separation region longer than that computed by Edwards and Carter [7]; however, in this case the present mesh is not considered fine enough for such a calculation and, also, the outlet boundary conditions are imposed at a not sufficiently downstream location. A very important point needs some attention: the solutions of Ref. 7 use a correct IBL model which contains the same terms of the NS equations considered by the present IBL-type approximation, when an appropriate, orthogonal

grid is employed. Therefore, for the present problem, the normal pressure gradient is indeed negligible in the (separated) boundary layer, but the present IBL-type model cannot be accurate insofar as it neglects the pressure gradient in the y direction, which is considerably inclined with respect to the direction normal to the wall, especially near the x = 0 and x =1 locations. In conclusion, the PNS equations can still be used in the presence of mild skewness of the computational mesh, but the IBL equations strictly require a body oriented coordinate mesh which is orthogonal, at least near the body surface.

As far as the efficiency of the calculations is concerned, the following points emerge: the present approach is reasonably efficient, but seems to require from two to four times more iterations than other current PNS or IBL solvers [7-10]. However, the present method is extremely robust, insofar a no parameter was ever optimized, or changed when solving the second more difficult problem, for which the convergence rate was found to be only marginally slower than for the first one (see Figures 7 and 9). Also, the present approach does not resort to any kind of inner iteration, insofar as the nonlinearities and the "elliptic" nature of the flow field are accounted by a single global iteration process. Furthermore, the present method is the only one which effectively employs second-order-accurate central differences for the first derivative in the streamwise direction and therefore is anticipated to be more accurate (for an equivalent mesh) to methods resorting to first-order-accurate upwind differences [8] or to the FLARE approximation in the separated region [7]. Finally, the convergence of the proposed approach can be improved by using backward sweeping (at least in the separated region) at successive iterations, horizontal line relaxations every once in a while, or a multigrid approach [19]. None of these possible improvements was employed here, because the aim of this work was by no means to provide the "most efficient" high Re weakly separated flow solver, but to demonstrate that the NS and PNS equations can be solved with essentially the same efficiency, so that it may be wise to consider all of the NS terms, in order to avoid unpleasant "surprises". From this respect, it is felt that such a goal has been achieved, together with the secondary ones of providing separated flow solutions to the classical BL equations, which are free of the separation singularity, and of assessing the influence of skewness in the computational mesh on the performance of PNS-type and IBL-type models.

References

1. Van Dyke, M., "Perturbation Methods in Fluid Mechanics", Parabolic Press, Stanford, CA.

2. Stewartson, K., "Multistructured boundary layers on flat plates and related bodies",

Advances in Appl. Mech., Vol. 14, 1974, p. 145.

3. Ghia, K. N., Ghia, U. and Tesch, W. A., "Evaluation of several approximate models for laminar incompressible separation by comparison with complete Navier-Stokes solutions", AGARD Conf. Proc., n. 168, 1975, p. 6-1.

4. Werle, M. J. and Bernstein, J. M., "A Comparative Numerical Study for Models of the Navier-Stokes Equations for Incompressible Separated Flows", AIAA Paper 75-48.

5. Catherall, D. and Mangler, K., "The integration of the two dimensional boundary-layer equations past a point of vanishing skin friction", J. Fluid Mech.. Vol. 26 1966, p.163.

6. Klineberg, J. and Steger, J., "On Laminar Boundary -Layer Separation", AIAA Paper 74-94.

7. Edwards, D. E. and Carter, J. E., "A Quasi-Simultaneous Finite Difference Approach for Strongly Interacting Flow", Third SNPAAF (Symposium on Numerical and Physical Aspects of Aerodynamic Flows), Long Beach, CA, Jan. 1985.

8. Halim, A. and Hafez, M., "Calculation of Separation Bubbles Using Boundary-Layer-Type Equations - Part I & II", AIAA Paper 84-1585.

9. Inoue, O.. "Separated Boundary Layer Flows with High Reynolds Numbers". Lecture Notes in Physics, Vol. 141, 1981, p. 224.

10. Hoffman, G. H., "Comparison of Parabolized Vorticity and Navier-Stokes Solutions in a Mildly Nonorthogonal Coordinate System", TM 82-72, The Penn. State University, 1982.

11. Smith, F. T., "The high Reynolds number theory of laminar flow", IMA J. of Appl. Math., Vol. 28, 1982, p. 207.

12. Cheng, H. K. and Smith, F. T., "The influence of airfoil thickness and Reynolds number on separation", ZAMP, Vol. 30, 1982, p. 151.

13. Cheng, H. K., "The Laminar Airfoil Beyond Trailing-Edge Stall, II", Third SNPAAF, Long Beach, CA, Jan. 1985.

14. Rothmayer, A. P. and Davis, R. T., "Massive Separation and Dynamic Stall on a Cusped Trailing-Edge Airfoil", Third SNPAAF, Long Beach, CA, Jan. 1985.

15. Roache, P. J., "Scaling of High Reynolds Number Weakly Separated Flows", First SNPAAF, Long Beach, CA, Jan. 1981.

16. Thompson, J. F., Thames, F. C. and Mastin, C. W., "Automatic Numerical Generation of Body Fitted Curvilinear Coordinate System for Fields Containing Any Number of Arbitrary Two-Dimensional Bodies", J. Comp. Phys., Vol. 15, 1974, p. 299.

17. Napolitano, M. and Walters, R. W., "An Incremental Block-Line-Gauss-Seidel Method for the Navier-Stokes Equations", AIAA Paper 85-0033.

18. Beam, R. M. and Warming, R. F., "An Implicit Factored Scheme for the Compressible Navier-Stokes Equations", AIAA Journal, Vol. 16, April 1978, p. 393.

19. Napolitano, M., "An Incremental Multigrid Strategy for the Fluid Dynamics Equations", Yale University Research Report, YALEU/DCS/RR-357.

Acknowledgements

The author is indebted to Dr. M. J. Werle, for many stimulating discussions and interesting suggestions. Discussions with Drs D. E. Edwards, J. E. Carter and M. Hafez were also valuable. The environment at the Research Center for Scientific Computation of Yale University, where most of this research was conducted, has been very beneficial to the outcome of this work.

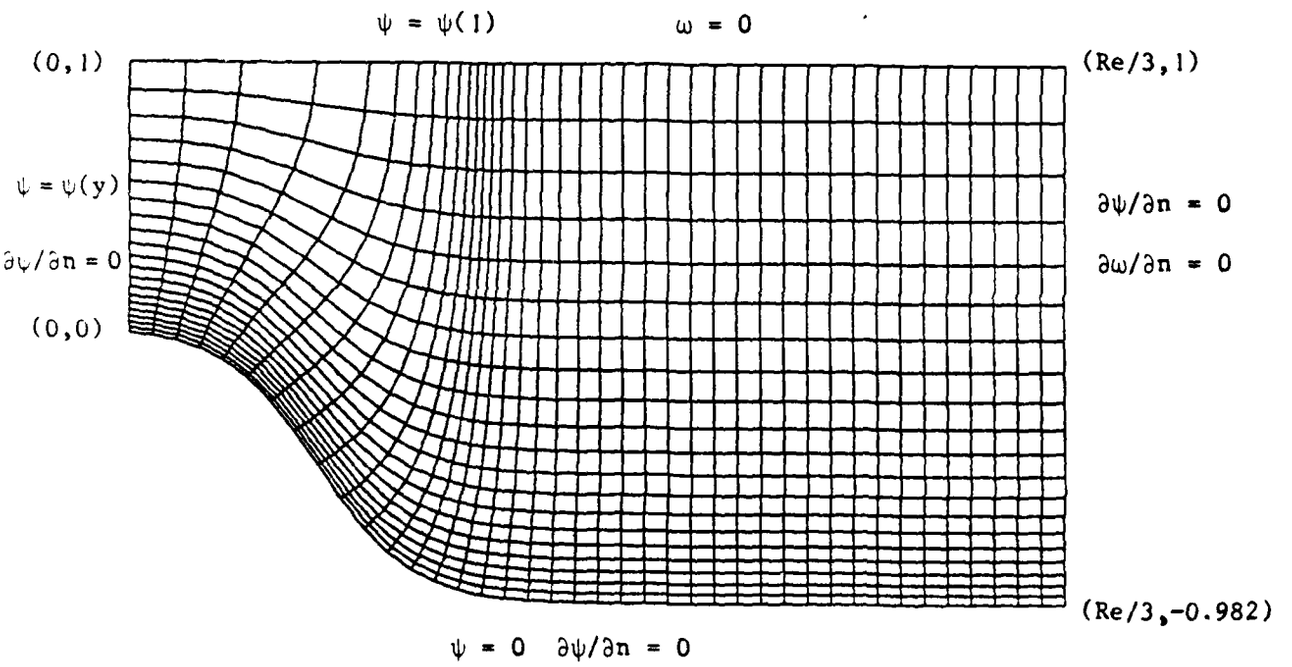

Figure 1. Channel flow geometry and mesh for Re = 10 and boundary conditions.

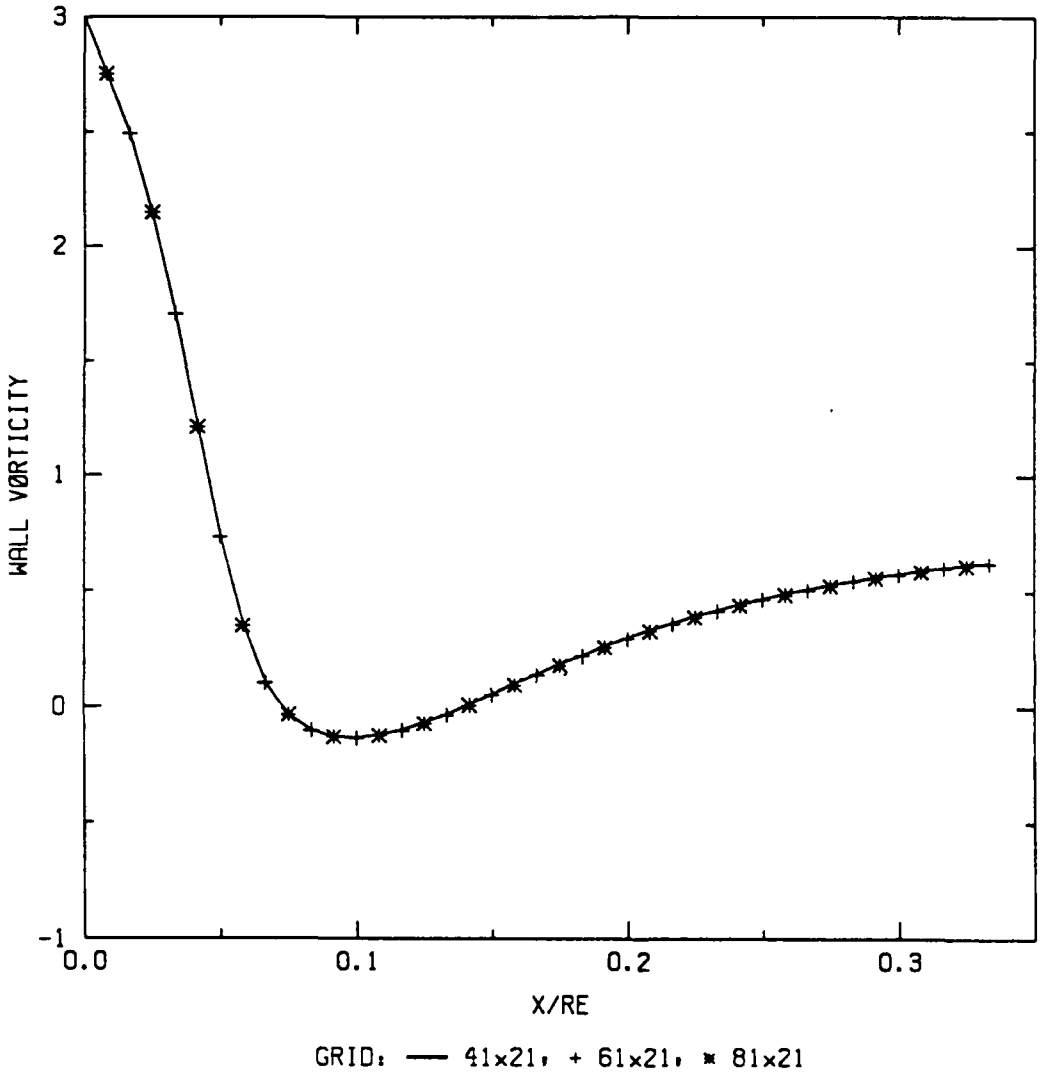

Figure 2. Longitudinal step size study for Re = 10^6 channel flow.

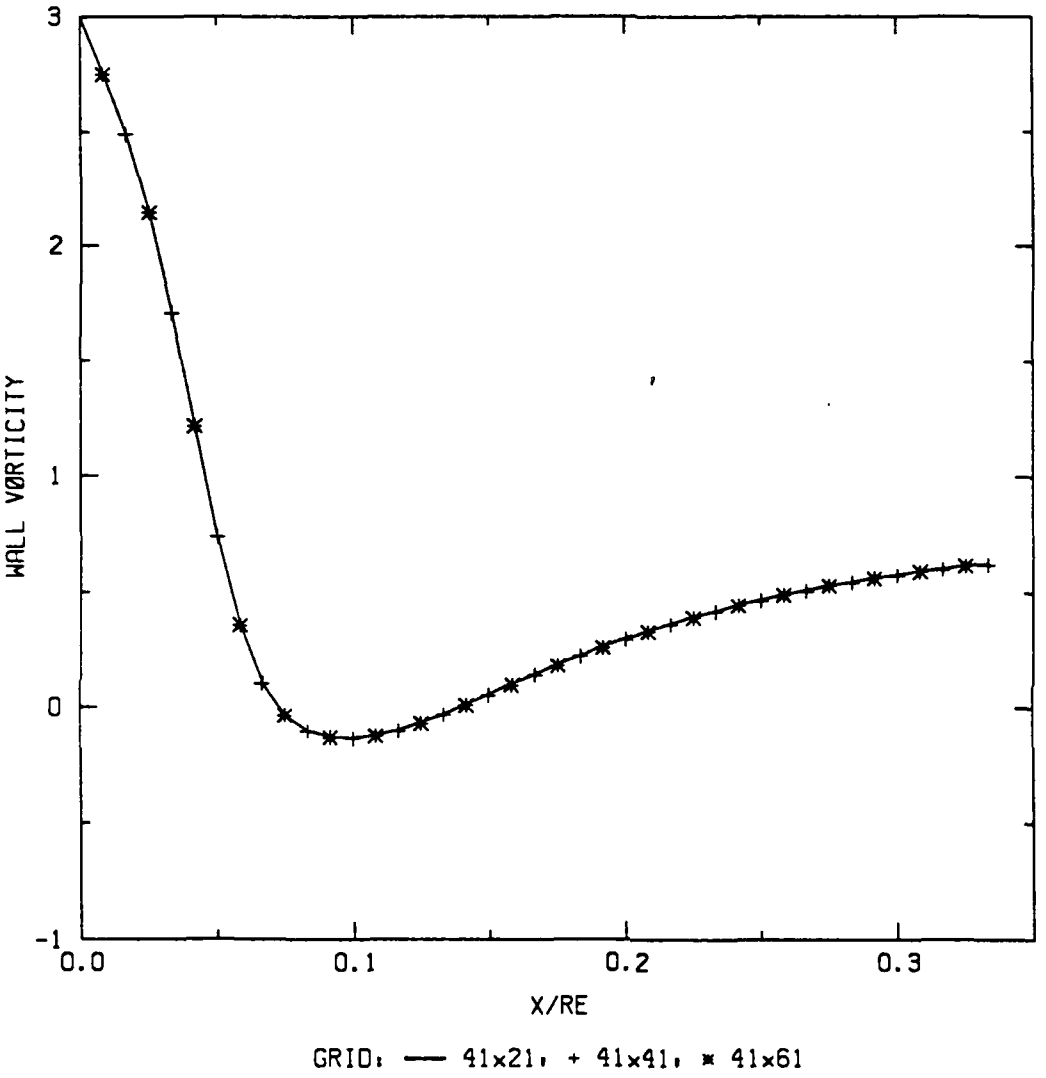

Figure 3. Transversal step size study for Re = 10^6 channel flow.

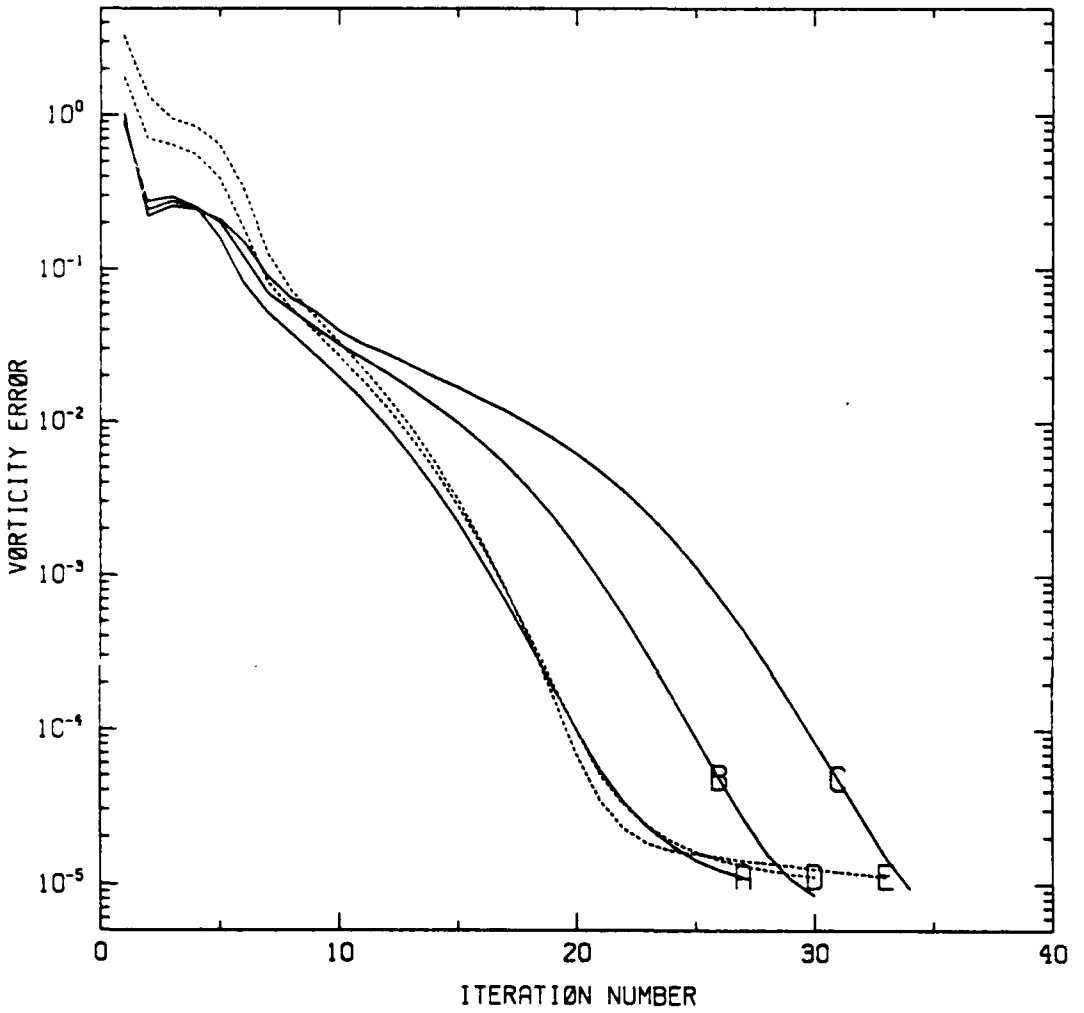

A - 41X21, B - 61X21, C - 81X21
D - 41X41, E - 41X61

Figure 4. Convergence history for Re = 10^6 channel flow.

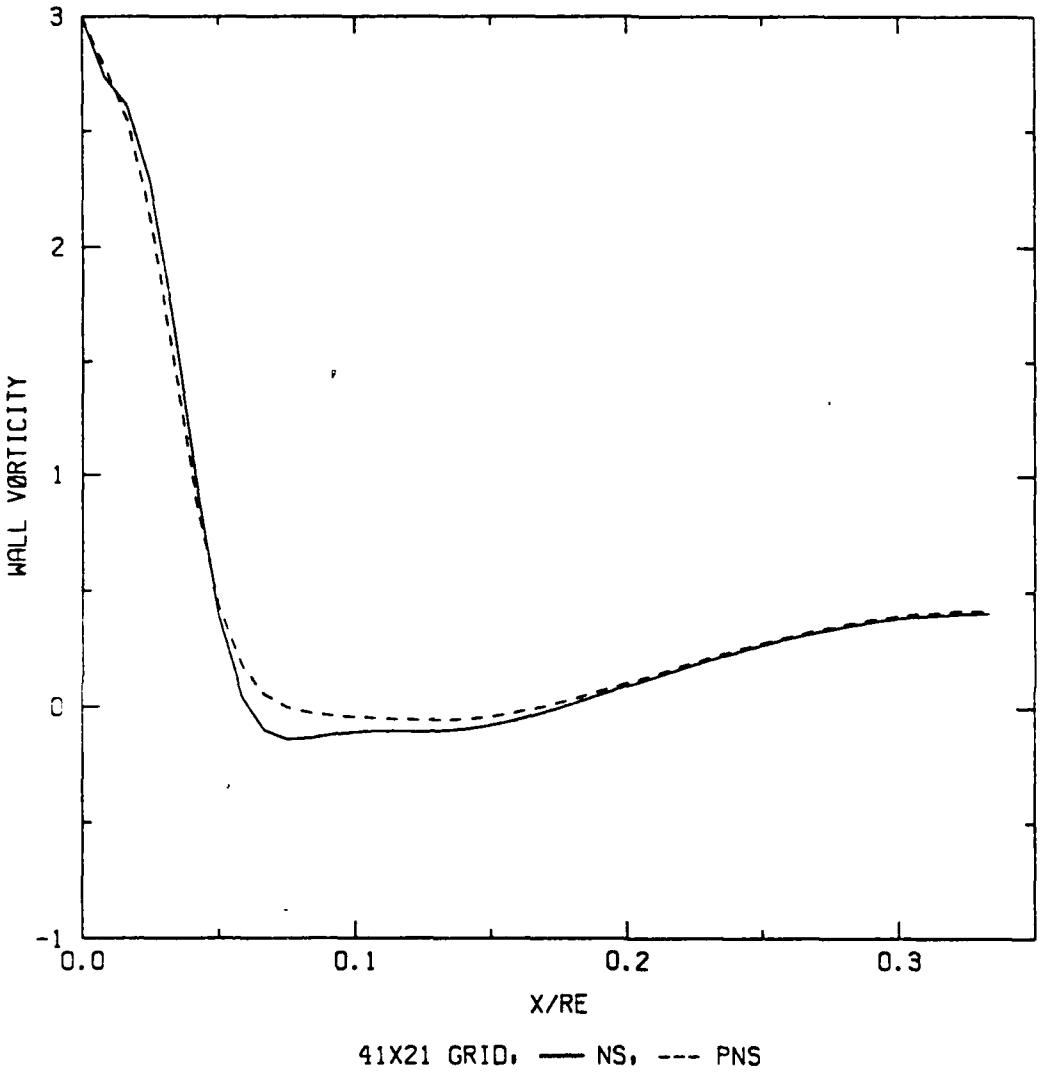

Figure 5. Comparison of NS and PNS results for Re = 10 channel flow.

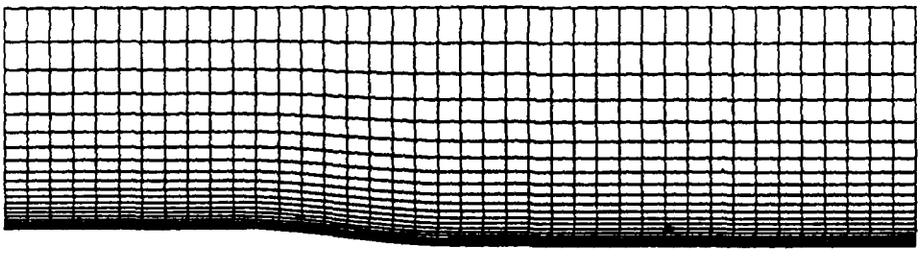

Figure 6a. Diffuser geometry and mesh for the case A = - 0.08.

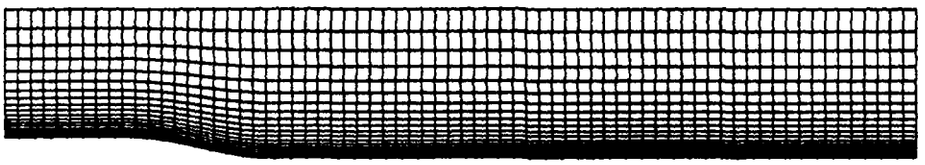

Figure 6b. Diffuser geometry and mesh for the case A = - 0.16.

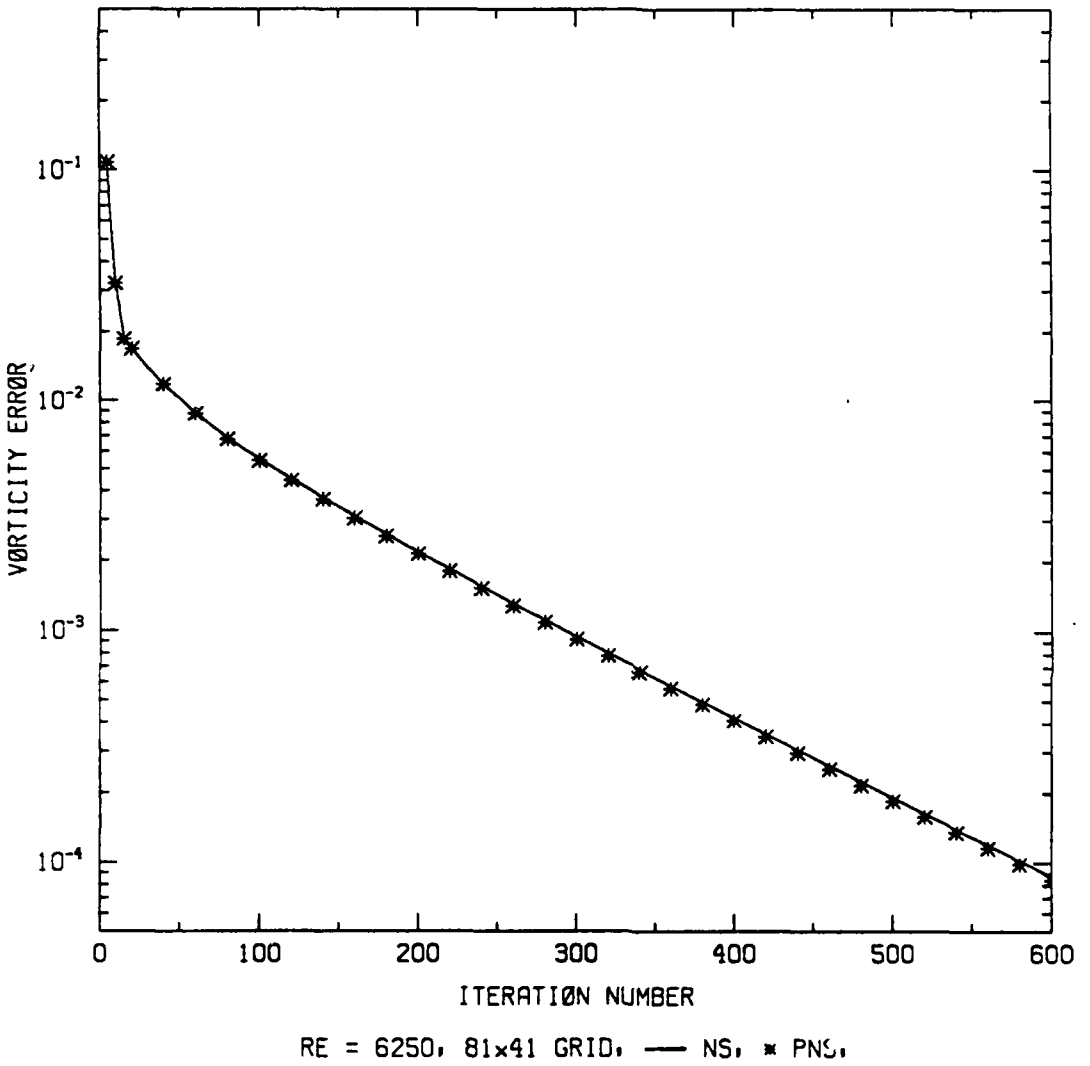

Figure 7. Convergence history for diffuser flow (Re = 6250; A = - 0.08).

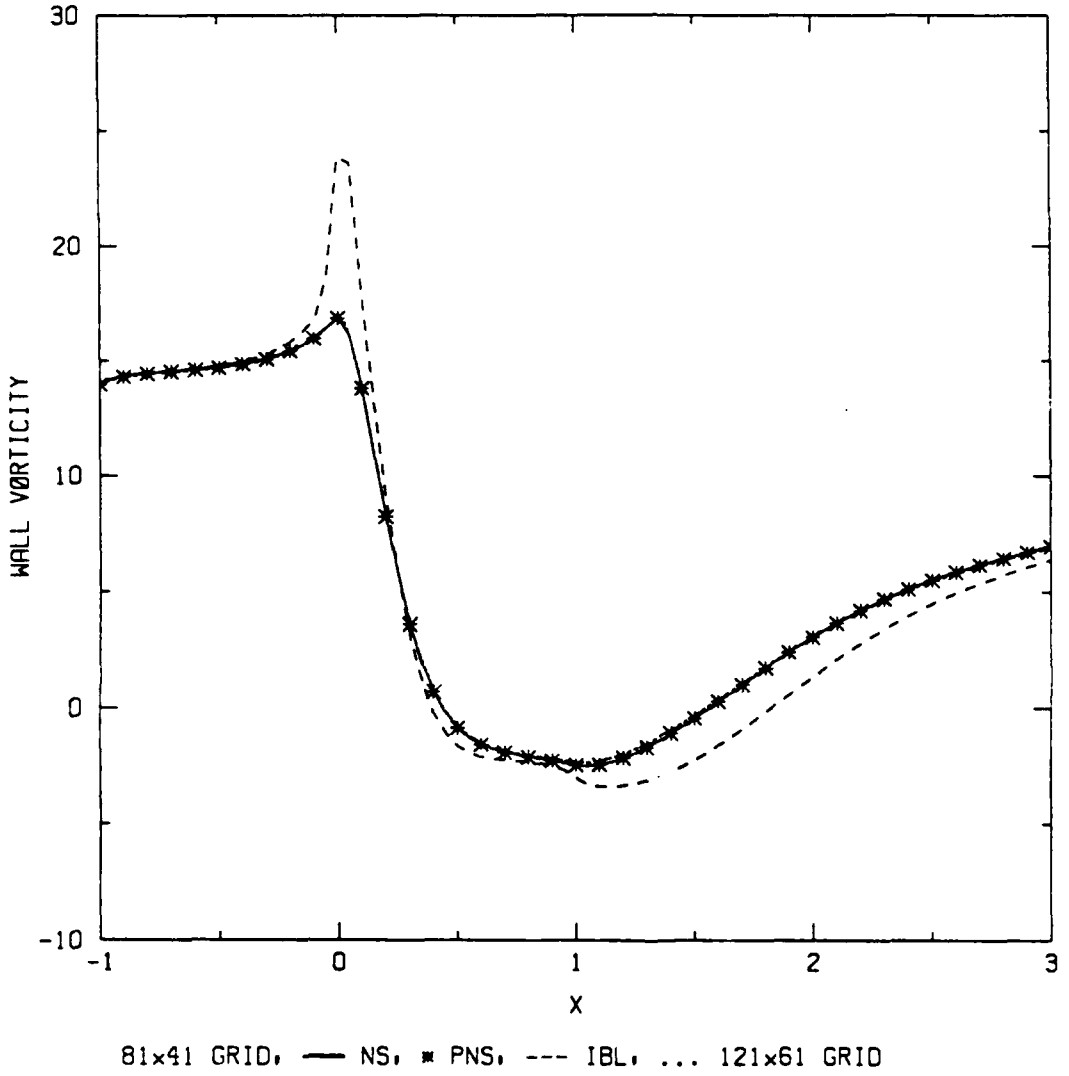

Figure 8. Wall vorticity results for diffuser flow (Re = 6250; A = - 0.08).

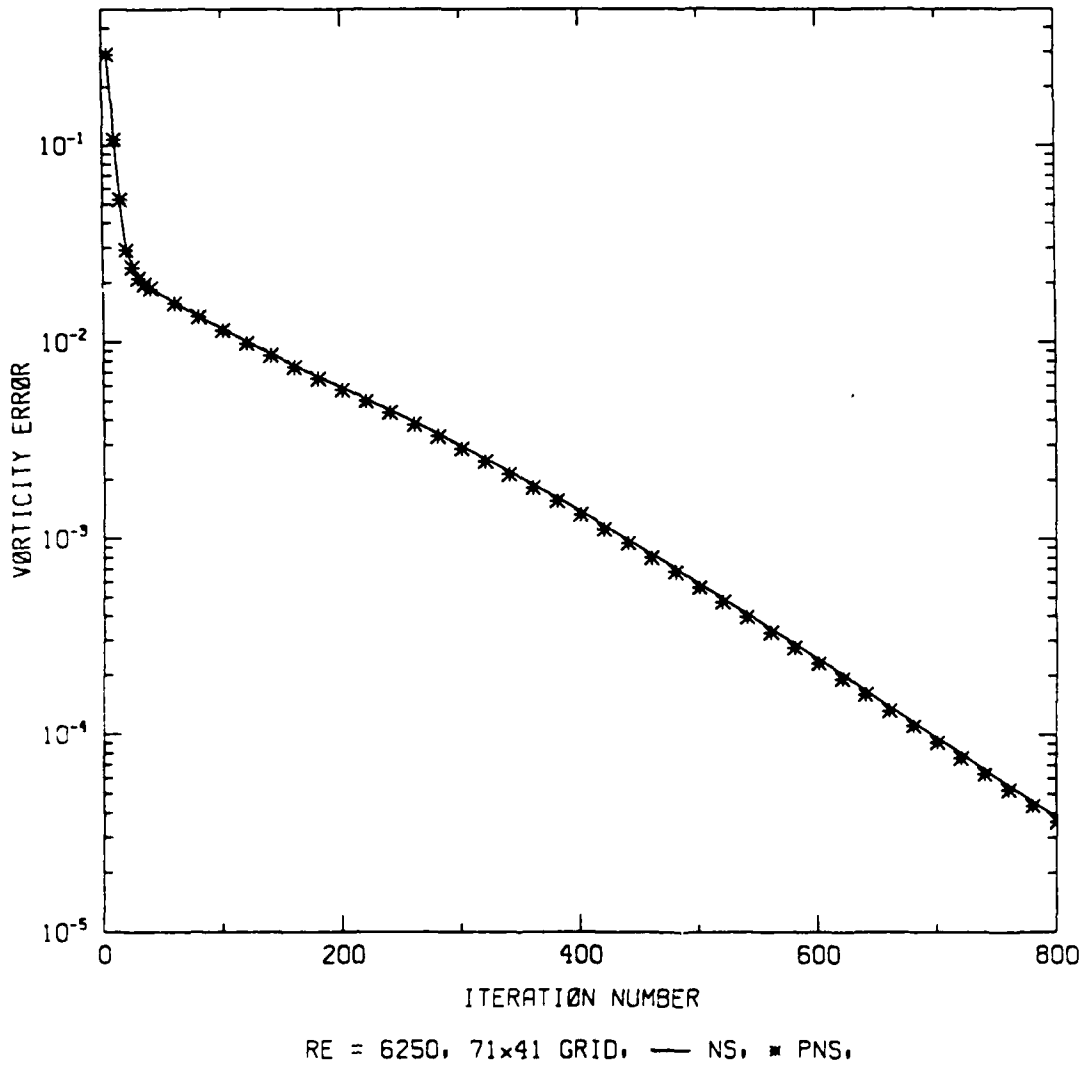

Figure 9. Convergence history for diffuser flow (Re = 6250; A = - 0.16).

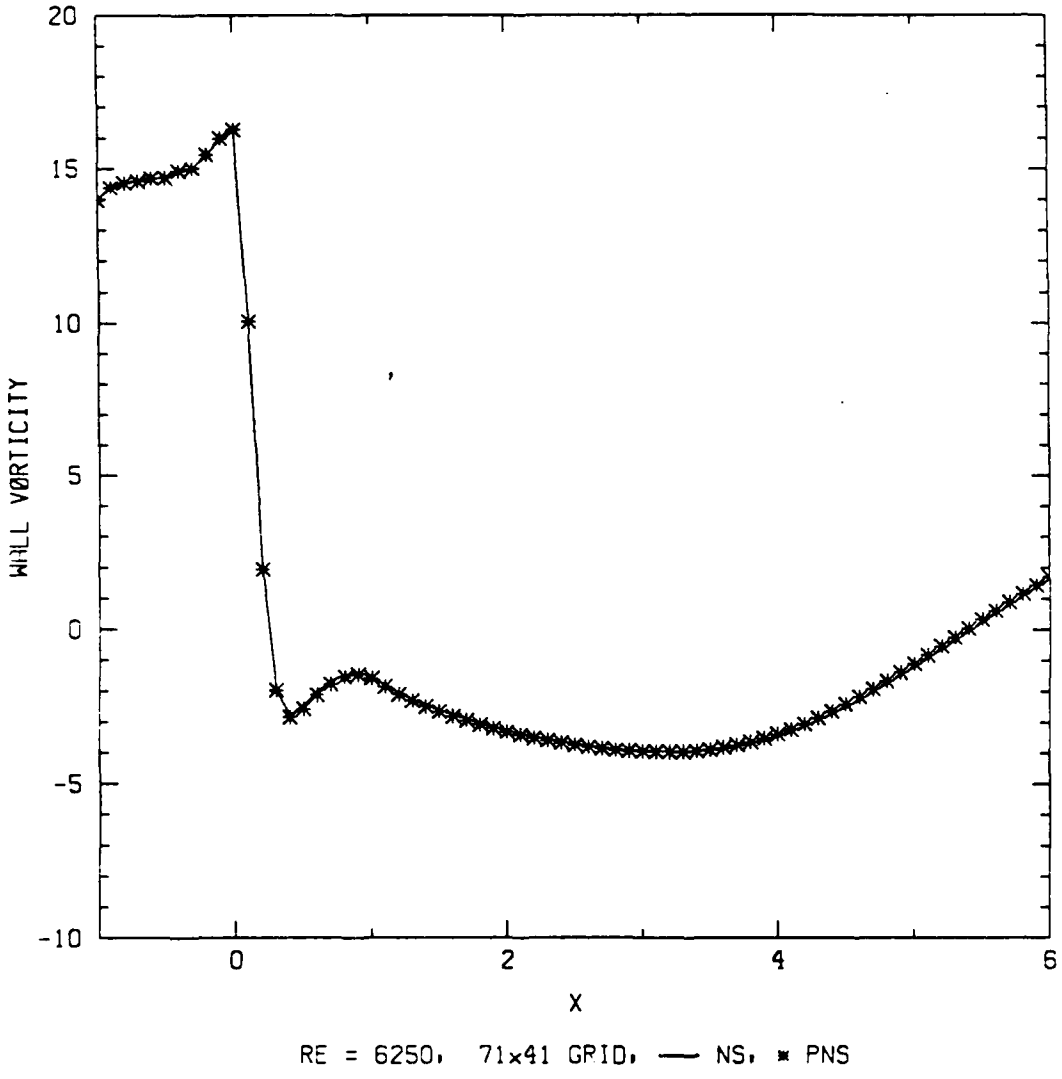

Figure 10. Wall vorticity results for diffuser flow (Re = 6250; A = - 0.16).

END

FILMED

5-85

DTIC